

# Multimodal Remote Inference

Keyuan Zhang\*, Yin Sun†, Bo Ji\*

\*Department of CS, Virginia Tech †Department of ECE, Auburn University  
Email: {keyuanz, boji}@vt.edu, yzs0078@auburn.edu

**Abstract**—We consider a remote inference system with multiple modalities, where a multimodal machine learning (ML) model performs real-time inference using features collected from remote sensors. As sensor observations may change dynamically over time, fresh features are critical for inference tasks. However, timely delivering features from all modalities is often infeasible due to limited network resources. To this end, we study a two-modality scheduling problem to minimize the ML model’s inference error, which is expressed as a penalty function of AoI for both modalities. We develop an index-based threshold policy and prove its optimality. Specifically, the scheduler switches modalities when the current modality’s index function exceeds a threshold. We show that the two modalities share the same threshold, and both the index functions and the threshold can be computed efficiently. The optimality of our policy holds for (i) general AoI functions that are *non-monotonic* and *non-additive* and (ii) *heterogeneous* transmission times. Numerical results show that our policy reduces inference error by up to 55% compared to round-robin and uniform random policies, which are oblivious to the AoI-based inference error function. Our results shed light on how to improve remote inference accuracy by optimizing task-oriented AoI functions.

**Index Terms**—Scheduling; Age of Information; Remote Inference; Multimodal

## I. INTRODUCTION

The advent of sixth-generation (6G) technology, along with advances in artificial intelligence (AI), enables *remote inference* in various intelligent applications, such as autonomous transportation, unmanned mobility, and industrial automation [1]. As illustrated in Fig. 1, a remote inference system uses AI models for inference tasks (e.g., monitoring, reasoning, and decision-making) based on features transmitted from remote sensors. For instance, traffic prediction relies on near real-time forecasts of traffic status (e.g., speed, flow, and demand) based on spatio-temporal road data [2]. When the sensor observations change dynamically over time, timely data delivery is critical. For example, autonomous driving requires timely updates on vehicle positions and velocities to ensure safety, and healthcare monitoring relies on real-time vital signs for timely alerts.

Moreover, many complex tasks involve multiple data modalities, such as audio, visual, 3D points (e.g., LiDAR or RADAR), and motion (e.g., IMU) data. Each modality provides complementary information to enhance the overall inference accuracy. Take object detection and tracking as an example: while color images (RGB) capture the shape and appearance of objects, LiDAR images offer depth information [3]. To fully exploit information from multiple modalities, machine

This work was supported in part by the National Science Foundation (NSF) under Grants CNS-2106427 and CNS-223967.

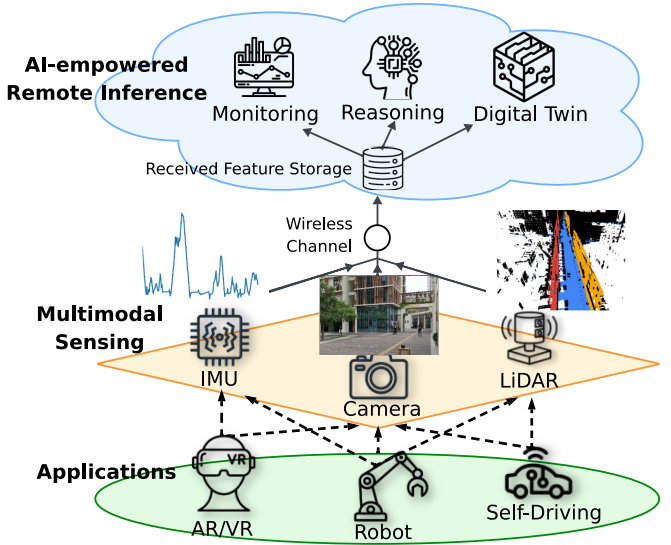


Fig. 1: A multimodal remote inference system.

learning (ML) based fusion techniques have been widely adopted, due to their effectiveness in extracting modality-specific information and capturing cross-modal correlations using architectures such as deep neural networks [4].

Despite the advantages of multimodal ML, its application in remote inference systems remains limited in practice. One primary challenge is limited network resources (e.g., bandwidth), which makes it hard for multimodal ML models to access fresh features across all modalities simultaneously. Therefore, it is important to schedule transmissions for the modality that contributes most to the ML model’s performance. Another challenge is the lack of a clear expression capturing the relationship between feature freshness and the ML model’s performance [5]. In other words, it is unclear which feature is most *valuable* to the model. One main reason is the complexity of multimodal ML models, especially deep neural networks.

To address these challenges, prior studies on remote inference have offered key insights into how information freshness affects ML performance [1], [6], [7]. In these studies, *Age of Information* (AoI), introduced in [8], serves as a crucial metric for evaluating freshness. A key finding from these works reveals that in supervised learning, ML inference error can be expressed as a function of AoI; surprisingly, this function need not be monotonic. This observation enables us to shift the goal from directly optimizing ML inference error to minimizing an AoI-based penalty function, which can be non-monotonic.

Moreover, the function depends on the AoIs of all modalities and may be non-additive, i.e., not a weighted sum of single-modality AoI functions (see Section V-C for an example). The generality of this function further complicates the scheduling problem.

Therefore, a key research question is the following: *Under limited network resources, how can we effectively schedule modalities to minimize the ML model's inference error?*

Our main contributions are summarized as follows:

- We formulate a two-modality scheduling problem aimed at minimizing inference error, which is a general function of the AoI of both modalities. The two-modality setting (e.g., visual-audio or RGB-LiDAR) is widely used in ML, but remains *underexplored* in remote inference.
- We develop an optimal *index-based threshold policy*. Specifically, one modality is scheduled continuously until its index function exceeds a threshold, and then the scheduler switches to the other modality. Interestingly, the two modalities share the same threshold. Both the index functions and the threshold can be computed efficiently. Our results apply to (i) general AoI functions that are *non-monotonic* and *non-additive* and (ii) *heterogeneous* modality transmission times.
- Numerical experiments on a robot state prediction task demonstrate that our policy reduces inference error by up to 55% compared to round-robin and uniform random policies, which are agnostic to inference error. These results shed light on how to improve remote inference accuracy by optimizing task-oriented AoI functions.

## II. RELATED WORK

**AoI penalty functions.** *Age of Information* is a widely adopted metric for quantifying information freshness. (see [1] and references therein, as well as a comprehensive survey [9]). Nevertheless, the relationship between information *freshness* and its *value* to the application is not well understood. To address this, in [10], Sun and Cyr suggested several non-decreasing, non-linear AoI functions to capture the value of fresh data in various applications. Researchers have also proposed various metrics, such as Age of Incorrect Information (AoII) [11], to quantify the value of information in different systems; see [12] for a comprehensive survey.

More recent research has explored the impact of freshness in remote inference systems. In the seminal work [6], [7], Shisher *et al.* demonstrated that inference error can be expressed as a general AoI penalty function, which may not be monotonic. Based on this observation, the authors studied a transmission scheduling problem to minimize a general AoI penalty function. In [13], the joint optimization of feature length selection and transmission scheduling was further studied. However, these prior works focus solely on the single-modality case, where each task corresponds to a single source. Optimizing a general AoI function for multiple modalities remains underexplored. We take a step forward by considering a general AoI function of two modalities. The new

objective adds an extra layer of complexity due to the non-separability of the two modalities.

**Multi-source AoI optimization.** There have also been efforts to optimize AoI in multi-source systems, such as queueing systems [14], broadcast networks [15], and remote inference systems [6], [7], [13]. In [14], Sun *et al.* studied age-optimal online scheduling in a multi-flow, multi-server queueing system, where the age function is time-dependent, symmetric, and non-decreasing. In [15], Kadota *et al.* demonstrated that the Maximum Age First (MAF) policy is optimal in a homogeneous network, and a suboptimal Whittle's index method was further applied for heterogeneous scenarios. In [13], Shisher *et al.* proposed the Net Gain policy for jointly optimizing feature length selection and source scheduling in multi-source scenarios. Although source and modality scheduling share similarities, our work considers a more general age function. Existing works on multi-source scheduling mostly consider an additive or a non-decreasing age function, whereas we consider a potentially non-monotonic and non-additive function. Therefore, approaches such as Whittle's index and Net Gain policy, which rely on the additive assumption, may not be directly applicable to our problem.

Additionally, this paper relates to scheduling for correlated sources. Prior studies in correlated sources often model the correlation explicitly, e.g., one source may contain another's information [16], [17]. In contrast, in our setting, the correlation among modalities is implicitly captured by the AoI-based penalty function, thus requiring a new algorithmic design.

## III. SYSTEM MODEL AND PROBLEM FORMULATION

Let  $\mathbb{R}$ ,  $\mathbb{N}$ , and  $\mathbb{Z}_+$  be the sets of real numbers, natural numbers, and positive integers, respectively.

### A. System Model

As depicted in Fig. 2, we consider a two-modality remote inference system, where two sensors send features to a receiver over a wireless channel. Each sensor corresponds to a distinct modality. Let time be slotted, indexed by  $t = 0, 1, 2, \dots$ . At each time  $t$ , each modality  $m$  generates one feature  $X_{m,t}$  from a given feature set  $\mathcal{X}_m$ ; the joint feature set is defined as  $\mathcal{X} := \mathcal{X}_1 \times \mathcal{X}_2$ . Meanwhile, on the receiver side, a predictor (e.g., a neural network) uses the *freshest received* features from both modalities to infer the current target value  $Y_t$  from a given target set  $\mathcal{Y}$ . Due to limited network resources, the scheduler can select one modality for transmission at any time. Suppose the  $n$ -th transmission starts at time  $S_n$  and completes at time  $D_n$ . At time  $S_n$ , the scheduler selects only one modality for transmission, and the decision is denoted by  $a_n \in \{1, 2\}$ . We assume that the scheduler always transmits the freshest feature, i.e.,  $X_{a_n, S_n}$ , from modality  $a_n$ .

Moreover, let  $T_m \in \mathbb{Z}_+$  denote the *fixed* transmission time for modality  $m$  ( $T_m < \infty$ ). Because of varying feature size,  $T_1$  and  $T_2$  may differ. The channel is reliable, and there is no preemption during transmission. That is, the receiver successfully receives the  $n$ -th selected feature from modality  $a_n$  at time  $D_n$ , and the transmission duration is  $T_{a_n}$ . When the

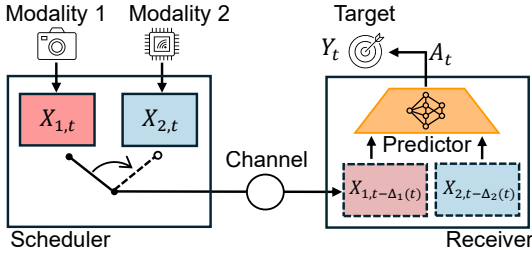


Fig. 2: System model.

current transmission completes, the next transmission begins immediately, i.e.,  $S_{n+1} = D_n$  for every  $n$ .

We use *age of information* to quantify information freshness, defined as the time elapsed since the freshest received feature was generated [18]. For each modality  $m$ , we denote its AoI at the receiver at time  $t$  as  $\Delta_m(t) \in \mathbb{Z}_+$ . According to the definition, the AoI of modality  $m$  at the receiver resets to its transmission time  $T_m$  whenever the receiver receives a feature from modality  $m$  (i.e.,  $a_n = m$  and  $t = D_n$  for some  $n$ ); otherwise, the AoI increases by 1. That is, the AoI of each modality  $m$  evolves as

$$\Delta_m(t) = \begin{cases} T_m & \text{if } a_n = m \text{ and } t = D_n, \\ \Delta_m(t-1) + 1 & \text{otherwise.} \end{cases} \quad (1)$$

The AoI vector of two modalities, denoted by  $\Delta(t)$ , is then defined as  $(\Delta_1(t), \Delta_2(t)) \in \mathbb{Z}_+^2$ .

a) *Inference error*: Define

$$\mathbf{X}_{t-\Delta(t)} := (X_{1,t-\Delta_1(t)}, X_{2,t-\Delta_2(t)}).$$

In order to predict the target  $Y_t \in \mathcal{Y}$ , the predictor  $\phi : \mathcal{X} \times \mathbb{Z}_+^2 \mapsto \mathcal{A}$  outputs an action  $A_t$  from a given action set  $\mathcal{A}$ ; the action is determined based on the freshest received features  $\mathbf{X}_{t-\Delta(t)} \in \mathcal{X}$  and the associated AoI vector  $\Delta(t) \in \mathbb{Z}_+^2$ . The performance of the prediction is evaluated using a loss function  $\ell(y, a)$ , which quantifies the inference error incurred if the predictor selects action  $a \in \mathcal{A}$  while the true target value is  $y \in \mathcal{Y}$ . For example, the action can be a probability distribution  $Q_Y$  in the space  $\mathcal{Y}$ , with the associated logarithmic loss function  $\ell_{\log}(y, Q_Y) := -\log Q_Y(y)$ . Alternatively, the action can be an estimate  $\hat{y} \in \mathcal{Y}$  of the true target value  $y \in \mathcal{Y}$ , with the associated quadratic loss function  $\ell_2(y, \hat{y}) := (y - \hat{y})^2$ .

We assume that the process  $\{(Y_t, X_t), t = 0, 1, 2, \dots\}$  is *stationary*. This indicates that the inference error is time-invariant. Second, the processes  $\{(Y_t, X_t), t = 0, 1, 2, \dots\}$  and  $\{\Delta(t), t = 0, 1, 2, \dots\}$  are *independent*. This holds when the scheduling policy does not know the feature or the target value (i.e., signal-agnostic). Under these two assumptions, the expected inference error at time  $t$  can be expressed as a function of the AoI vector [7]. Specifically, we use  $L : \mathbb{Z}_+^2 \mapsto \mathbb{R}$  to denote the expected inference error function. For every AoI vector  $\delta$ , function  $L(\delta)$  is defined as

$$L(\delta) := \mathbb{E}_{Y, \mathbf{X} \sim \mathbb{P}(Y_t, \mathbf{X}_{t-\Delta(t)})} [\ell(Y, \phi(\mathbf{X}, \delta))],$$

where  $\mathbb{P}(Y_t, \mathbf{X}_{t-\Delta(t)})$  denotes the joint stationary distribution of the target and the feature used for inference. The function

$L$  can be quite general; we only require it to be uniformly bounded, as stated below:

**Assumption 1** (Uniformly Bounded  $L$ ). *There exists a finite constant  $M$  such that  $|L(\delta)| \leq M$  for every AoI vector  $\delta$ .*

Assumption 1 ensures the existence of an optimal policy in our analysis; this is also practical as ML models commonly apply preprocessing techniques to keep loss bounded.

b) *Scheduling policy*: The policy  $\pi$  is represented as a sequence of modality choices, i.e.,  $\pi := (a_0, a_1, a_2, \dots)$ . We focus on scheduling policies that satisfy three conditions. (i) *Signal-agnostic*: The scheduler does not know the signal value (i.e., the feature or the target value) at any time. This is practical when the task-related signals are private to the scheduler. (ii) *Causal*: Each decision  $a_n$  relies solely on the current and historical AoI at the receiver (i.e.,  $\Delta(0), \Delta(1), \dots, \Delta(S_n)$ ) (iii) The scheduler knows the expected inference error function  $L$ . In practice, this function can be numerically estimated by calculating the average loss over the dataset for each AoI vector. Let  $\Pi$  denote the set of all policies satisfying these conditions.

### B. Problem Formulation

We aim to find a scheduling policy in  $\Pi$  that minimizes the time-averaged expected inference error over an infinite horizon. We define this problem as Problem **OPT**:

$$\text{OPT} \quad \bar{L}_{\text{opt}} := \inf_{\pi \in \Pi} \limsup_{T \rightarrow \infty} \frac{1}{T} \mathbb{E}_{\pi} \left[ \sum_{t=0}^{T-1} L(\Delta(t)) \right].$$

### IV. OPTIMAL SCHEDULING POLICY DESIGN

The roadmap for this section is as follows. We first reformulate the problem and cast it as a Semi-Markov Decision Process (SMDP); the reformulated problem is simpler to solve. Then, we present our policy and prove its optimality. More interpretations of our policy are provided at the end.

### A. Problem Reformulation

At first glance, the problem requires selecting a modality at each delivery time. We next show that it can be reduced to two decisions, each associated with a special state.

Define two special AoI states, called *restart states*:  $\Delta_{1,\text{re}} := (T_1, T_1 + T_2)$  and  $\Delta_{2,\text{re}} := (T_1 + T_2, T_2)$ . Define  $m'$  as the complementary modality of modality  $m$ , that is,  $m' \in \{1, 2\} \setminus \{m\}$ . At each restart state  $\Delta_{m,\text{re}}$ , the scheduler determines the number of consecutive transmissions of modality  $m$  before switching to modality  $m'$ , denoted by  $\tau_m \in \mathbb{N}$ . That is, the scheduler selects modality  $m$  for  $\tau_m$  consecutive transmissions, followed by one transmission from modality  $m'$ . It turns out that the process always restarts at state  $\Delta_{m',\text{re}}$ , regardless of the value of the decision  $\tau_m$ . This is because, according to the AoI evolution in Eq. (1), upon the delivery of the transmission from modality  $m'$ , the AoI of modality  $m'$  resets to  $T_{m'}$ , while the AoI of modality  $m$  increases to  $T_m + T_{m'}$ . Fig. 3 illustrates an example of the process under unit transmission times (i.e.,  $T_1 = T_2 = 1$ ).

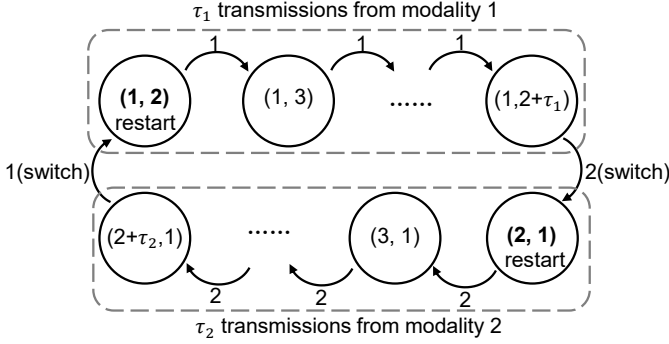


Fig. 3: An example of AoI transitions under unit transmission times ( $T_1 = T_2 = 1$ ). Each circle represents an AoI vector, and the number on each arrow represents the decision, i.e., the selected modality. The restart states are  $(1, 2)$  and  $(2, 1)$ .

We cast the above process as a Semi-Markov Decision Process (SMDP). The process has two states  $\Delta_{m,\text{re}}, \Delta_{m',\text{re}} \in \mathbb{Z}_+^2$ . At state  $\Delta_{m,\text{re}}$ , the scheduler takes an action  $\tau_m \in \mathbb{N}$ . That is, it selects modality  $m$  for  $\tau_m$  consecutive times, then switches to modality  $m'$  (with one transmission from  $m'$ ). The transition probability from  $\Delta_{m,\text{re}}$  to  $\Delta_{m',\text{re}}$  equals 1, i.e., the process switches between two states. The transition duration is given by  $\tau_m T_m + T_{m'}$ . Let  $C_m(\tau)$  denote the transition cost when the action  $\tau_m = \tau$ . For modality 1, we have

$$C_1(\tau) = \sum_{j=1}^{\tau} \sum_{i=0}^{T_1-1} L(T_1 + i, jT_1 + T_2 + i) + \sum_{i=0}^{T_2-1} L(T_1 + i, (\tau + 1)T_1 + T_2 + i),$$

which represents the total inference error during  $\tau$  transmissions from modality 1 and one transmission from modality 2. Similarly, for modality 2, we have

$$C_2(\tau) = \sum_{j=1}^{\tau} \sum_{i=0}^{T_2-1} L(T_1 + jT_2 + i, T_2 + i) + \sum_{i=0}^{T_1-1} L(T_1 + (\tau + 1)T_2 + i, T_2 + i).$$

The objective is to minimize the cycle inference error, i.e.,

$$\inf_{\tau_1, \tau_2 \in \mathbb{N}} \frac{C_1(\tau_1) + C_2(\tau_2)}{(\tau_1 + 1)T_1 + (\tau_2 + 1)T_2}. \quad (2)$$

Let  $h(\cdot)$  denote the relative value function. The Bellman optimality equation is given by

$$h(\Delta_{m,\text{re}}) = \inf_{\tau_m \in \mathbb{N}} [C_m(\tau_m) - (\tau_m T_m + T_{m'}) \bar{L}_{\text{opt}} + h(\Delta_{m',\text{re}})], \quad \forall m = 1, 2. \quad (3)$$

According to [19, Prop. 7.4.1], if the process returns to the restart state within finite time under all policies, optimizing Problem **OPT** is equivalent to optimizing the cycle inference error in Eq. (2). As the AoI evolution is deterministic, it

suffices to find the optimal solution  $\tau_m$ . We focus on policies with finite  $\tau_m$  for each  $m$ , which ensure the process returns to a restart state in finite time.

While dynamic programming methods (e.g., policy or value iteration) can solve the Bellman optimality equation (3), they suffer from the curse of dimensionality. We next present a low-complexity method to determine the optimal solution.

### B. Optimal Policy

Before presenting the optimal policy, we define the index function. For every  $\theta \in \mathbb{N}$ , the index function of modality  $m$ , denoted by  $\gamma_m$ , is defined as

$$\gamma_m(\theta) := \inf_{k \in \mathbb{Z}_+} \frac{C_m(\theta + k) - C_m(\theta)}{kT_m}, \quad (4)$$

where the numerator is the additional total inference error and the denominator is the additional transition duration, both when  $\tau_m$  is  $\theta + k$  instead of  $\theta$  (see Remark 1 in Section IV-D for a detailed explanation of the index function).

**Theorem 1.** Suppose  $L$  is uniformly bounded (Assumption 1). For every  $\beta \in \mathbb{R}$ , define

$$\tau_{m,\text{opt}}(\beta) = \inf\{\theta \in \mathbb{N} : \gamma_m(\theta) \geq \beta\}, \quad \forall m \in \{1, 2\}, \quad (5)$$

where the index function  $\gamma_m$  of each modality  $m$  is defined in Eq. (4). An optimal policy for Problem **OPT**, represented by  $\tau_{m,\text{opt}}$  for each  $m \in \{1, 2\}$ , is then given by

$$\tau_{m,\text{opt}} = \tau_{m,\text{opt}}(\bar{L}_{\text{opt}}) = \inf\{\theta \in \mathbb{N} : \gamma_m(\theta) \geq \bar{L}_{\text{opt}}\}, \quad (6)$$

where the threshold  $\bar{L}_{\text{opt}}$  is the optimal objective value of Problem **OPT**. To determine  $\bar{L}_{\text{opt}}$ , define two functions

$$g_1(\beta) := C_1(\tau_{1,\text{opt}}(\beta)) + C_2(\tau_{2,\text{opt}}(\beta)),$$

$$g_2(\beta) := (\tau_{1,\text{opt}}(\beta) + 1)T_1 + (\tau_{2,\text{opt}}(\beta) + 1)T_2.$$

The threshold  $\bar{L}_{\text{opt}}$  is a root of

$$g_1(\beta) - \beta g_2(\beta) = 0. \quad (7)$$

We will prove the theorem in Section IV-C. Eq. (5) suggests that the optimal policy exhibits an *index-based threshold* structure. That is, the policy selects modality  $m$  for  $\theta$  consecutive transmissions, stopping at the first time when the index function  $\gamma_m(\theta)$  exceeds a threshold  $\beta$ . Then the policy switches to select the other modality. The index function for each modality can be pre-computed independently, as it depends only on the known parameters (i.e., the inference error function and the transmission times).

Moreover, Eq. (6) shows that, under the optimal policy, both modalities share the same threshold  $\bar{L}_{\text{opt}}$ , which is exactly the optimal objective value of Problem **OPT**. The threshold  $\bar{L}_{\text{opt}}$  can be determined by solving Eq. (7). As will be shown later, Eq. (7) is obtained by substituting  $\beta$  and  $\tau_{m,\text{opt}}(\beta)$  into the Bellman optimality equation (3). The following proposition shows that Eq. (7) can be efficiently solved.

### Proposition 1. Define

$$g(\beta) := g_1(\beta) - \beta g_2(\beta). \quad (8)$$

The function  $g$  has the following properties:

- (i)  $g$  is concave, continuous, and strictly decreasing,
- (ii)  $\lim_{\beta \rightarrow \infty} g(\beta) = -\infty$  and  $\lim_{\beta \rightarrow -\infty} g(\beta) = \infty$ .

*Proof sketch:* The function  $g$  is the left-hand side of Eq. (7). It can be shown that  $g$  is essentially the infimum of multiple linear functions of  $\beta$  with negative coefficients, which leads to the properties stated above. The complete proof is similar to that of [1, Lemma 9] and is therefore omitted. ■

Given these properties of  $g$ , we can efficiently solve Eq. (7) (i.e.,  $g(\beta) = 0$ ) using low-complexity algorithms such as bisection search and Newton's method [20, Algorithm 1-3].

### C. Proof of Theorem 1

We prove Theorem 1 by showing that our policy satisfies the Bellman optimality equation (3) and the optimal solution  $\tau_{m,\text{opt}}$  attains the infimum in Eq. (3) for every  $m$ . According to average-cost MDP theory [19, Proposition 4.2.1], if there exists a finite scalar  $\bar{L}_{\text{opt}}$  and a uniformly bounded function  $h$  that solves the Bellman optimality equation, then an optimal policy exists. Furthermore, a policy is optimal if it attains the infimum in the Bellman optimality equation for all states.

We cannot directly solve each equation independently, because the optimal objective value  $\bar{L}_{\text{opt}}$  appears in the Bellman optimality equation (3) for each state  $\Delta_{m,\text{re}}$ . To this end, we fix  $\bar{L}_{\text{opt}} = \beta$  for arbitrary  $\beta \in \mathbb{R}$ , and focus on solving Problem **OPT**- $\beta$ , defined as

$$\mathbf{OPT}\text{-}\beta \quad \inf_{\tau \in \mathbb{N}} [C_m(\tau) - \tau T_m \beta], \quad \forall m \in \{1, 2\}.$$

From the Bellman optimality equation (3) to Problem **OPT**- $\beta$ , we discard two terms:  $T_{m'} \bar{L}_{\text{opt}}$  and  $h(\Delta_{m',\text{re}})$ , as they are independent of the decision  $\tau_m$ . Note that Problem **OPT**- $\beta$  can be solved separately for each modality. The next proposition shows that the optimal solution for Problem **OPT**- $\beta$  can be expressed in terms of  $\beta$ .

**Proposition 2.** Suppose  $L$  is uniformly bounded (Assumption 1). For every given  $\beta$  and  $m$ , the optimal solution to Problem **OPT**- $\beta$  is given by  $\tau_{m,\text{opt}}(\beta)$  in Eq. (5), i.e.,

$$\tau_{m,\text{opt}}(\beta) = \inf \{\theta \in \mathbb{N} : \gamma_m(\theta) \geq \beta\},$$

where the index function  $\gamma_m$  is defined in Eq. (4).

*Proof sketch:* We use induction to show that  $\tau_{m,\text{opt}}(\beta) = \theta$  attains the infimum of Problem **OPT**- $\beta$  if it satisfies Eq. (5). Firstly, we show that  $\tau_{m,\text{opt}}(\beta) = 0$  if  $\gamma_m(0) \geq \beta$ . Then, assume that the  $\tau_{m,\text{opt}}(\beta)$  satisfies Eq. (5) when  $\tau_{m,\text{opt}}(\beta) = 0, 1, \dots, \theta - 1$ . We can show that  $\tau_{m,\text{opt}}(\beta) = \theta$  if (i)  $\gamma_m(i) < \beta$  for  $i = 0, 1, \dots, \theta - 1$  and (ii)  $\gamma_m(\theta) \geq \beta$ . Combining conditions (i) and (ii), we derive Eq. (5). See the Appendix for the detailed proof. ■

Proposition 2 shows that the optimal solution  $\tau_{m,\text{opt}}(\beta)$  for Problem **OPT**- $\beta$  attains the infimum in the Bellman optimality equation (3) when  $\bar{L}_{\text{opt}} = \beta$ . Hence,  $\tau_{m,\text{opt}}(\bar{L}_{\text{opt}})$  given in Eq. (6) is an optimal policy for Problem **OPT**.

Next, we show that  $\bar{L}_{\text{opt}}$  is a root of Eq. (7) by constructing a solution to the Bellman optimality equation (3). We substitute  $\bar{L}_{\text{opt}} = \beta$  and  $\tau_{m,\text{opt}}(\beta)$  into the Bellman optimality equation (3) and obtain

$$h(\Delta_{m,\text{re}})$$

$$= C_m(\tau_{m,\text{opt}}(\beta)) - (\tau_{m,\text{opt}}(\beta) T_m + T_{m'}) \beta + h(\Delta_{m',\text{re}}),$$

for each modality  $m$ . Let  $h(\Delta_{m',\text{re}}) = 0$ , we have

$$h(\Delta_{m,\text{re}}) = C_m(\tau_{m,\text{opt}}(\beta)) - (\tau_{m,\text{opt}}(\beta) T_m + T_{m'}) \beta,$$

$$0 = C_{m'}(\tau_{m',\text{opt}}(\beta)) - (\tau_{m',\text{opt}}(\beta) T_{m'} + T_m) \beta + h(\Delta_{m,\text{re}}).$$

By summing the two equations, canceling  $h(\Delta_{m,\text{re}})$ , and rearranging the terms, we obtain a function of  $\beta$ :

$$C_m(\tau_{m',\text{opt}}(\beta)) + C_{m'}(\tau_{m',\text{opt}}(\beta))$$

$$- \beta[(\tau_{m,\text{opt}}(\beta) + 1) T_m + (\tau_{m',\text{opt}}(\beta) + 1) T_{m'}] = 0,$$

which is exactly Eq. (7) in Theorem 1. Finally, we show that  $\bar{L}_{\text{opt}}$  and  $h(\Delta_{m,\text{re}})$  exist and are bounded, which concludes the proof of Theorem 1. With the two properties stated in Proposition 2 and by applying the Intermediate Value Theorem [21], we conclude that Eq. (7) has a unique and finite root. Thus,  $\bar{L}_{\text{opt}}$  exists and is finite. By substituting  $\tau_{m,\text{opt}}(\bar{L}_{\text{opt}})$  and  $h(\Delta_{m',\text{re}}) = 0$  into the Bellman optimality equation, we obtain  $h(\Delta_{m,\text{re}})$ . Furthermore,  $h(\Delta_{m,\text{re}})$  is bounded because  $\bar{L}_{\text{opt}}$ ,  $\tau_{m,\text{opt}}$ ,  $T_m$ , and  $L$  are bounded. ■

### D. Discussions

We explain the meaning of the index function in Remark 1 and highlight how our index-based threshold policy generalizes and relates to prior work in Remarks 2 and 3.

**Remark 1.** The index function  $\gamma_m(\theta)$  reflects the **minimum future cost** if the scheduler continues to select modality  $m$  after having selected it for  $\theta$  consecutive transmissions. To see this, consider a symmetric case when  $T_1 = T_2 = T_c$  for some constant  $T_c \in \mathbb{Z}_+$ . Then, the index function for modality 1 in Eq. (5) becomes

$$\gamma_1(\theta) = \inf_{k \in \mathbb{Z}_+} \frac{\sum_{j=1}^k \sum_{i=0}^{T_c-1} L(T_c + i, (\theta + 2 + j)T_c + i)}{kT_c},$$

which calculates the minimum average cost starting from the AoI state  $(T_c, (\theta + 3)T_c)$  (i.e., when  $j = 1$ ) until switching. Furthermore, our index function also handles the asymmetric case. Specifically, suppose  $T_1 > T_2$ . Define

$$C_a(\theta, k) := \sum_{j=1}^{k-1} \sum_{i=0}^{T_1-1} L(T_1 + i, (\theta + 1 + j)T_1 + T_2 + i),$$

$$C_b(\theta, k) := \sum_{i=0}^{T_2-1} L(T_1 + i, (\theta + k + 1)T_1 + T_2 + i) + \sum_{i=T_2}^{T_1-1} L(T_1 + i, (\theta + 2)T_2 + i).$$

The index function for modality 1 then becomes

$$\gamma_1(\theta) = \inf_{k \in \mathbb{Z}_+} \frac{C_a(\theta, k) + C_b(\theta, k)}{kT_1},$$

where  $C_a(\theta, k)$  quantifies the total future cost and  $C_b(\theta, k)$  adjusts the cost due to different transmission times.

**Remark 2.** Our results generalize the two-source scheduling in remote estimation [22]. Specifically, when the inference error function  $L$  is non-decreasing and the two modalities have unit transmission times (i.e.,  $T_1 = T_2 = 1$ ), the index function of modality 1 reduces to

$$\gamma_1(\theta) = \inf_{k \in \mathbb{Z}_+} \frac{\sum_{j=\theta+2}^{\theta+k+1} L(1, j+1)}{k} = L(1, \theta+3),$$

where the last equality holds as the infimum is achieved when  $k = 1$  as  $L$  is non-decreasing. Then, the optimal policy for modality 1 is  $\tau_{1,\text{opt}} = \inf\{\theta : L(1, \theta+3) \geq \bar{L}_{\text{opt}}\}$ , which can be shown to be equivalent to the result in [22, Proposition 3.5]. Note that in this special case, the index function is non-decreasing, whereas in our setting, it can be non-monotonic.

**Remark 3.** A similar index-based threshold policy has been studied in the single-source scheduling for remote inference [1], [13]. Specifically, under stationary random transmission time, the optimal time to send a new feature is when an AoI-based index function exceeds a threshold. In contrast, we apply the index function to the optimal modality scheduling problem, which differs from the single-source setting.

## V. NUMERICAL CASE STUDY: ROBOT STATE PREDICTION

In this section, we examine our multimodal remote inference system through a case study on robot state prediction and conduct a trace-driven evaluation to assess our policy.

### A. System Description

Consider a robot performing tasks such as lifting objects or walking. It gathers both environmental and self-state information using multimodal sensors, such as LiDAR, cameras, and onboard sensors. On the receiver side, a predictor aims to continuously track the robot's state, such as its pose and velocity. A transmitter sends the features collected from the robot to the receiver, where an ML model is used to predict the robot's state based on the received data. Due to the high dimensionality and varying sizes of the data, transmission often spans multiple time slots and may differ across modalities. Next, we describe our experimental setup.

### B. Experimental Setup

We consider the OpenAI Bipedal Walker as our robot task, where a four-joint robot must run over stumps, pitfalls, and other obstacles (see [23] for details). The reinforcement learning algorithm used to control the robot is TD3-FORK [24], which achieves state-of-the-art performance on this task. After training the control model, we generate a time-series dataset in the OpenAI Gymnasium simulation environment, consisting of LiDAR rangefinder measurements, robot state information, and joint control signals.

For the state prediction task, we aim to predict the robot's joint velocities using sequential LiDAR measurements and joint control signals as two distinct modalities. We adopt the

Long Short-Term Memory (LSTM) neural network as the predictor model, due to its widespread use and effectiveness in time-series forecasting. The network architecture includes an input layer, a hidden layer with 20 LSTM cells, and a fully connected output layer. We use 80% of the dataset for training. To incorporate AoI into model training, we augment the dataset as follows: given any AoI vector  $(\delta_1, \delta_2)$ , we construct the feature-label pairs  $(X_{1,t-\delta_1}, X_{2,t-\delta_2}; Y_t)$  for all data points, where the input features are aligned with their corresponding AoI values. The LSTM network takes the AoI vector as two additional input features and is trained on the augmented training dataset.

All experiments were run on a server with an AMD EPYC 7313 CPU (16 cores) and a single NVIDIA A2 GPU.

### C. The Impact of AoI on Inference Error

Fig. 4 illustrates how the inference error varies with the AoI for two modalities, with each AoI ranging from 1 to 50. The color intensity or surface height represents the expected inference error on the testing dataset. Although the inference error generally increases with the AoI of either modality, the function is not monotonic. Furthermore, the impact of each modality differs significantly: as the AoI of modality 1 (LiDAR) increases, the inference error grows significantly faster than it does for modality 2 (control signal). It indicates that LiDAR data is more strongly correlated with the target signal. Moreover, the figure suggests that the inference error may not be an additive function of the AoI vector; the effect of one modality's AoI on the inference error depends on the AoI of the other modality. Overall, the empirical results show that the inference error may be a non-monotonic and non-additive function of the AoI vector.

### D. Scheduling Policies Evaluation

We compare the following scheduling policies:

- (i) Index-based threshold policy: This is our policy, as described in Theorem 1.
- (ii) Round-robin policy: This policy alternates between the two modalities. Notably, this policy is optimal for minimizing the sum of AoI, i.e.,  $L(\Delta(t)) = \sum_{m=1}^2 \Delta_m(t)$ .
- (iii) Uniform random policy: The policy randomly selects one of the two modalities with equal probability, regardless of the current AoI state.

We use the results obtained in Section V-C as the empirical expected inference error function of the AoI vector. We vary the transmission time for each modality, taking values 2, 4, 6, 8, 10, to reflect different feature sizes. Fig. 5 presents the performance of each scheduling policy under varying transmission times. Our proposed index policy consistently achieves the best performance across all cases, reducing the inference error by up to 53% compared to the randomized policy and up to 55% compared to the round-robin policy. Although the round-robin policy is effective for minimizing AoI, it fails to capture the complex relationship between inference error and AoI, leading to suboptimal performance in certain scenarios (e.g., when  $T_1 = 2$  and  $T_2 = 10$ ).

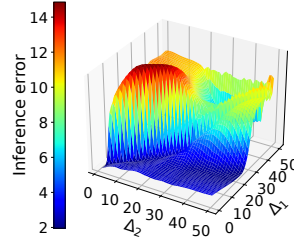
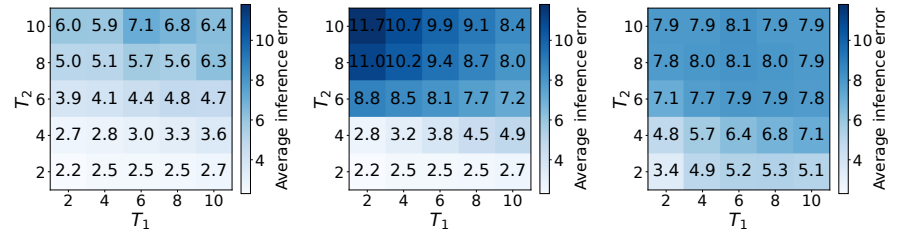


Fig. 4: Inference error vs. AoI.



(a) Index policy (ours)

(b) Round-robin

(c) Uniform random

Fig. 5: Performance comparison under varying transmission times.

The uniform random policy exhibits similar limitations, as it ignores both inference error and AoI. These results underscore the importance of jointly considering both modalities and their impact on inference error when designing scheduling policies.

## VI. CONCLUSION AND FUTURE WORK

We studied the two-modality scheduling problem for remote inference systems, where a receiver-side ML model relies on time-sensitive data from remote sensors. We derived an optimal policy applicable to general AoI penalty functions and heterogeneous transmission times. Experiments on robot state prediction show that our policy reduces inference error by up to 55% compared to baselines.

One future direction is to extend the proposed index-based threshold policy beyond two coupled modalities to general multimodal settings. The extension is non-trivial due to the *curse of dimensionality*, as the state space grows exponentially with more modalities. Another direction is to relax the current assumptions of reliable communication and deterministic transmission times. Considering unreliable channels and random delays would make the model more practical, but also add significant complexity to policy design. Last but not least, we assume that ML inference error is a time-invariant AoI function. Optimizing a time-dependent AoI function is essential for applications with complex, non-stationary dynamics.

## REFERENCES

- [1] M. K. C. Shisher, Y. Sun, and I.-H. Hou, “Timely communications for remote inference,” *IEEE/ACM Transactions on Networking*, vol. 32, no. 5, pp. 3824–3839, 2024.
- [2] H. Yuan and G. Li, “A survey of traffic prediction: from spatio-temporal data to intelligent transportation,” *Data Science and Engineering*, vol. 6, no. 1, pp. 63–85, 2021.
- [3] A. Asvadi, P. Girão, P. Peixoto, and U. Nunes, “3d object tracking using rgb and lidar data,” in *IEEE ITSC*, 2016, pp. 1255–1260.
- [4] P. P. Liang, A. Zadeh, and L.-P. Morency, “Foundations & trends in multimodal machine learning: Principles, challenges, and open questions,” *ACM Comput. Surv.*, vol. 56, no. 10, pp. 1–42, Jun. 2024.
- [5] A. Li, S. Wu, G. C. Lee, and S. Sun, “From freshness to effectiveness: Goal-oriented sampling for remote decision making,” *arXiv preprint arXiv:2504.19507*, 2025.
- [6] M. K. Chowdhury Shisher, H. Qin, L. Yang, F. Yan, and Y. Sun, “The age of correlated features in supervised learning based forecasting,” in *IEEE INFOCOM Workshops*, 2021, pp. 1–8.
- [7] M. K. C. Shisher and Y. Sun, “How does data freshness affect real-time supervised learning?” in *ACM MobiHoc*, 2022, p. 31–40.
- [8] S. Kaul, R. Yates, and M. Gruteser, “Real-time status: How often should one update?” in *IEEE INFOCOM*, 2012, pp. 2731–2735.
- [9] R. D. Yates, Y. Sun, D. R. Brown, S. K. Kaul, E. Modiano, and S. Ulukus, “Age of information: An introduction and survey,” *IEEE Journal on Selected Areas in Communications*, vol. 39, no. 5, pp. 1183–1210, 2021.
- [10] Y. Sun and B. Cyr, “Sampling for data freshness optimization: Non-linear age functions,” *Journal of Communications and Networks*, vol. 21, no. 3, pp. 204–219, 2019.
- [11] A. Maatouk, S. Kriouile, M. Assaad, and A. Ephremides, “The age of incorrect information: A new performance metric for status updates,” *IEEE/ACM Trans. Netw.*, vol. 28, no. 5, p. 2215–2228, 2020.
- [12] A. Li, S. Wu, S. Meng, R. Lu, S. Sun, and Q. Zhang, “Toward goal-oriented semantic communications: New metrics, framework, and open challenges,” *IEEE Wireless Communications*, vol. 31, no. 5, pp. 238–245, 2024.
- [13] M. K. C. Shisher, B. Ji, I.-H. Hou, and Y. Sun, “Learning and communications co-design for remote inference systems: Feature length selection and transmission scheduling,” *IEEE Journal on Selected Areas in Information Theory*, pp. 524–538, 2023.
- [14] Y. Sun, E. Uysal-Biyikoglu, and S. Komella, “Age-optimal updates of multiple information flows,” in *IEEE INFOCOM Workshops*, 2018, pp. 136–141.
- [15] I. Kadota, E. Uysal-Biyikoglu, R. Singh, and E. Modiano, “Minimizing the age of information in broadcast wireless networks,” in *54th Allerton*, 2016, pp. 844–851.
- [16] V. Tripathi and E. Modiano, “Optimizing age of information with correlated sources,” *IEEE/ACM Transactions on Networking*, vol. 32, no. 6, pp. 4660–4675, 2024.
- [17] B. Zhou and W. Saad, “On the age of information in internet of things systems with correlated devices,” in *IEEE GLOBECOM*, 2020, pp. 1–6.
- [18] Y. Sun, E. Uysal-Biyikoglu, R. D. Yates, C. E. Koksal, and N. B. Shroff, “Update or wait: How to keep your data fresh,” *IEEE Transactions on Information Theory*, vol. 63, no. 11, pp. 7492–7508, 2017.
- [19] D. P. Bertsekas, *Dynamic Programming and Optimal Control*, 3rd ed. Athena Scientific, 2005, vol. I.
- [20] T. Z. Ornee and Y. Sun, “Sampling and remote estimation for the ornstein-uhlenbeck process through queues: Age of information and beyond,” *IEEE/ACM Transactions on Networking*, vol. 29, no. 5, pp. 1962–1975, 2021.
- [21] R. G. Bartle and D. R. Sherbert, *Introduction to real analysis*, 4th ed. Wiley, 2011.
- [22] L. Shi and H. Zhang, “Scheduling two gauss–markov systems: An optimal solution for remote state estimation under bandwidth constraint,” *IEEE Trans on Signal Processing*, vol. 60, no. 4, pp. 2038–2042, 2012.
- [23] M. Towers, A. Kwiatkowski, J. Terry, J. U. Balis, G. De Cola, T. Deleu, M. Goulão, A. Kallinteris, M. Krimmel, A. KG *et al.*, “Gymnasium: A standard interface for reinforcement learning environments,” *arXiv preprint arXiv:2407.17032*, 2024.
- [24] H. Wei and L. Ying, “Fork: A forward-looking actor for model-free reinforcement learning,” in *IEEE CDC*, 2021, pp. 1554–1559.

APPENDIX  
PROOF OF PROPOSITION 2

Recall two definitions. For every  $\beta$ , Problem **OPT**- $\beta$  is

$$\inf_{\tau \in \mathbb{N}} [C_m(\tau) - \tau T_m \beta], \quad \forall m \in \{1, 2\}.$$

The index function  $\gamma_m$  of modality  $m$ , defined in Eq. (4), is

$$\gamma_m(\theta) = \inf_{k \in \mathbb{Z}_+} \frac{C_m(\theta + k) - C_m(\theta)}{k T_m}.$$

For every given  $\beta$  and  $m$ , let  $\tau_{m,\text{opt}}(\beta)$  denote the optimal solution that attains the infimum of Problem **OPT**- $\beta$ . Our goal is to show that  $\tau_{m,\text{opt}}(\beta)$  satisfies Eq. (5), i.e.,

$$\tau_{m,\text{opt}}(\beta) = \inf\{\theta \in \mathbb{N} : \gamma_m(\theta) \geq \beta\}.$$

Throughout the proof, we assume that the infimum in Eq. (5) exists. Otherwise, we have  $\gamma_m(\theta) \leq \beta$  for all  $\theta$ , which implies  $\tau_{m,\text{opt}}(\beta) = \infty$ ; this case is not considered in this paper.

We proceed by induction. That is, we aim to show that for all  $i \in \mathbb{N}$ , if  $i = \inf\{\theta \in \mathbb{N} : \gamma_m(\theta) \geq \beta\}$ , then  $\tau_{m,\text{opt}}(\beta) = i$ . First, we show the base case when  $i = 0$ . From the definition of  $\gamma_m$ , we have

$$\gamma_m(0) = \inf_{k \in \{1, 2, \dots\}} \frac{C_m(k) - C_m(0)}{k T_m} \geq \beta.$$

By rearranging terms, we obtain

$$\inf_{k \in \{1, 2, \dots\}} \left[ \frac{C_m(k) - C_m(0)}{k T_m} - \beta \right] \geq 0.$$

Because  $k T_m > 0$ , multiplying both sides by  $k T_m$  yields

$$\inf_{k \in \{1, 2, \dots\}} [C_m(k) - C_m(0) - k T_m \beta] \geq 0.$$

As  $C_m(0)$  is independent of  $k$ , pulling it out yields

$$\inf_{k \in \{1, 2, \dots\}} [C_m(k) - k T_m \beta] \geq C_m(0). \quad (9)$$

The left-hand side (LHS) of Eq. (9) is the infimum of Problem **OPT**- $\beta$  over  $\tau \in \{1, 2, \dots\}$ ; and its right-hand side (RHS) is the objective value of **OPT**- $\beta$  when  $\tau = 0$ . Hence, Eq. (9) implies that  $\tau_{m,\text{opt}}(\beta) = 0$ .

For an arbitrary  $j \geq 1$ , assume that the result holds for  $i = 0, 1, \dots, j-1$ . We now show that  $\tau_{m,\text{opt}}(\beta) = j$  if

$$j = \inf\{\theta \in \mathbb{N} : \gamma_m(\theta) \geq \beta\}. \quad (10)$$

Eq. (10) is equivalent to the following two conditions:

- (i)  $\gamma_m(i) < \beta$  for  $i = 0, 1, \dots, j-1$ ;
- (ii)  $\gamma_m(j) \geq \beta$ .

From condition (i), we aim to show that  $\tau_{m,\text{opt}}(\beta) \geq j$  by contradiction. Suppose  $\tau_{m,\text{opt}}(\beta) = i$  for some  $i < j$ . By the induction hypothesis, we have  $i = \inf\{\theta \in \mathbb{N} : \gamma_m(\theta) \geq \beta\}$ . Hence,  $\gamma_m(i) \geq \beta$ , contradicting condition (i).

From condition (ii), we aim to show that  $\tau_{m,\text{opt}}(\beta) \leq j$ . From the definition of  $\gamma_m$ , we have

$$\gamma_m(j) = \inf_{k \in \{1, 2, \dots\}} \frac{C_m(j+k) - C_m(j)}{k T_m} \geq \beta.$$

Multiplying both sides by  $k T_m$  and rearranging terms yields

$$\inf_{k \in \{1, 2, \dots\}} [C_m(j+k) - k T_m \beta] \geq C_m(j).$$

Subtracting  $j T_m \beta$  from both sides yields

$$\inf_{k \in \{1, 2, \dots\}} [C_m(j+k) - (j+k) T_m \beta] \geq C_m(j) - j T_m \beta. \quad (11)$$

Replacing  $j+k$  with  $\tau$ , the LHS of Eq. (11) is equivalent to

$$\inf_{\tau \in \{j+1, j+2, \dots\}} [C_m(\tau) - \tau T_m \beta].$$

The RHS of Eq. (11) is the objective value of Problem **OPT**- $\beta$  when  $\tau = j$ . Hence, Eq. (11) implies that  $\tau_{m,\text{opt}}(\beta) \leq j$ .

Combining  $\tau_{m,\text{opt}}(\beta) \geq j$  and  $\tau_{m,\text{opt}}(\beta) \leq j$ , we conclude that  $\tau_{m,\text{opt}}(\beta) = j$ . This completes the induction. ■